Reservoir characterization in Under-balanced Drilling using Low-Order Lumped Model

Amirhossein Nikoofard[a,*], Tor Arne Johansen[a], Glenn-Ole Kaasa[b,a]

[a] *Department of Engineering Cybernetics, Norwegian University of Science and Technology, 7491 Trondheim,Norway*
[b] *Kelda Drilling Controls*

Abstract

Estimation of the production index of oil and gas from the reservoir into the well during Under-Balanced Drilling (UBD) is studied. This paper compares a Lyapunov-based adaptive observer and a joint unscented Kalman filter (UKF) based on a low order lumped (LOL) model and the joint UKF based on the distributed drift-flux model by using real-time measurements of the choke and the bottom-hole pressures. Using the OLGA simulator, it is found that all adaptive observers are capable of identifying the production constants of gas and liquid from the reservoir into the well, with some differences in performance. The results show that the LOL model is sufficient for the purpose of reservoir characterization during UBD operations. Robustness of the adaptive observers is investigated in case of uncertainties and errors in the reservoir and well parameters of the models.

Keywords: Lyapunov-based Adaptive Observer, OLGA simulator, Low-order lumped model, Under-balanced drilling, UKF, Drift-flux model

1. Introduction

Since the number of depleted formations and cost of field exploration and development has increased, for the past two decades there has been increasing interest in new technology and automation of the drilling process which can improve drilling efficiency and increase oil recovery. UBD is a technology that enables drilling with the downhole pressure lower than the pore pressure of the formation. UBD has several advantages compared to conventional drilling in increasing the ultimate recovery from the reservoir, reducing the non-productive time (NPT), minimizing the risk of lost circulation, increasing the rate of penetration (ROP), reducing drilling-fluid costs through the use of cheaper, lighter fluid systems, and reducing drilling problems such as hole cleaning and differential sticking [1, 2].

*Corresponding author
Email addresses: Amirhossein.nikoofard@ntnu.no (Amirhossein Nikoofard), Tor.arne.johansen@itk.ntnu.no (Tor Arne Johansen), gok@kelda.no (Glenn-Ole Kaasa)

Real-time updates of reservoir properties may improve efficiency of the overall well construction by more accurate reservoir characterization while drilling, ultimately enabling increased oil recovery by better well completion. Reservoir characterization during UBD has been investigated by several researchers[3, 4, 5, 6, 7], focusing mainly on the estimation of the reservoir pore pressure and reservoir permeability by using the assumption that the total flow rate from the reservoir is known [5]. Kneissl proposed an algorithm to estimate both reservoir pore pressure and reservoir permeability during UBD while performing an excitation of the bottom-hole pressure [4]. However, the variations of fluid flow behavior in the downhole and the annuls section might introduce significant uncertainties to estimation of the reservoir pore pressure. Vefring et al. [5, 6] compared and evaluated the performance of the ensemble Kalman filter and an off-line nonlinear least squares technique utilizing the Levenberg-Marquardt optimization algorithm to estimate reservoir pore pressure and reservoir permeability during UBD while performing an excitation of the bottom-hole pressure. The result shows that excitation of the bottom-hole pressure might improve the estimation of the reservoir pore pressure and reservoir permeability [5, 6]. Gao Li et al. presented an algorithm for characterizing reservoir pore pressure and reservoir permeability during UBD of horizontal wells [7]. Since the total flow rate from the reservoir has a negative linear correlation with the bottom hole pressure, reservoir pore pressure can be identified by the crossing of the horizontal axis and the best-fit regression line between the total flow rate from the reservoir and the bottom hole pressure while performing an excitation of the bottom-hole pressure by changing the choke valve opening or pump rates.

In this paper, it is assumed that reservoir pore pressure is known by identification using Li's method [7] or other algorithms. The main focus is to estimate both production constants of gas and liquid during UBD operations, simultaneously. Due to the complexity of the multiphase flow dynamics of a UBD well coupled with a reservoir, the modeling, estimation and control of UBD operations is still considered an emerging and challenging topic in drilling automation. Nygaard et al. compared and evaluated the performance of the extended Kalman filter, the ensemble Kalman filter and the unscented Kalman filter based on a low order model to estimate the states and the production index (PI) in UBD operation [8]. Lorentzen et al. designed an ensemble Kalman filter based on a drift-flux model to tune the uncertain parameters of a two-phase flow model in the UBD operation [9]. In Nygaard et al. [10], a finite horizon nonlinear model predictive control in combination with an unscented Kalman filter was designed for controlling the bottom-hole pressure based on a low order model developed in [11], and the unscented Kalman filter (UKF) was used to estimate the states, and the friction and choke coefficients. A Nonlinear Moving Horizon Observer based on a low-order lumped model (LOL) was designed for estimating the total mass of gas and liquid in the annulus and geological properties of the reservoir during UBD operation for pipe connection procedure in [12]. Aarsnes et al. introduced a simplified drift-flux model and estimation of the distributed multiphase dynamics during UBD operation. This model used a specific empirical slip law without flow-regime predictions [13]. The estimation algorithm separates slowly varying parameters and potentially more quickly changing parameters such as the PI. Fast changing parameters are estimated online simultaneously with the states of the model, but other parameters are calibrated infrequently and offline. Nikoofard et al.

designed an UKF for estimation of unmeasured states, production and slip parameters of simplified drift-flux model using real time measurements of the bottom-hole pressure and liquid and gas rate at the outlet [14]. Di Meglio et al. designed an adaptive observer based on a backstepping approach for a linear first-order hyperbolic system of Partial Differential Equations (PDEs) by using only boundary measurements with application to UBD [15]. It is shown that this method has exponential convergence for the distributed state and the parameter estimation. This adaptive observer is applied to estimate distributed states and unknown boundary parameters of the well during UBD operations. Nikoofard et al. designed Lyapunov-based adaptive observer, a recursive least squares estimator and a UKF based on a LOL model to estimate states and parameters during UBD operations. For this estimation the total mass of gas and liquid was used as measurements. These values were calculated from pressure measurements using the LOL model [16]. In [16], the performance of the adaptive estimators was compared and evaluated for pipe connection procedure using a simple simulation model. In [17] the extended version of adaptive observer used in [16] was directly using real-time measurements of the choke and the bottom-hole pressures to estimate states and parameters. The performance of the adaptive observers was compared and evaluated for typical drilling case to estimate only production constant of gas using a simulated scenario with drift-flux model. In the present paper, the adaptive observers from [17] is compared and evaluated for an UBD case study to estimate both production constants of gas and liquid using some simulated scenarios with the OLGA simulator. The OLGA dynamic multiphase flow simulator is a high fidelity simulation tool which has become the de facto industry standard in oil and gas production, see [18]. These adaptive observers were tested by two challenging scenarios:

1. Changing for production constant of gas.
2. Pipe connection.

The performance of the estimation algorithms to detect and track the change in production parameters is investigated in a more realistic setting.

Lyapunov based adaptive observers and the Kalman filter are widely used for the estimation of state and parameters. A Lyapunov based adaptive observer is generally designed as Luenberger type observer for the state combined with an appropriate adaptive law to estimate the unknown parameters [19]. The unscented Kalman filter (UKF) has been shown to typically have a better performance than other Kalman filter techniques for nonlinear system [20, 21].

The purpose of the paper is to evaluate the LOL model for reservoir characterization in UBD employing an adaptive observer that uses the bottom hole and choke pressure measurements from a simulated scenario with the OLGA simulator. This paper presents the design of a Lyapunov-based adaptive observer and an UKF based on LOL model, and an UKF based on a simplified drift-flux model, to estimate the states and geological properties of the reservoir (production parameters) during UBD operation. The performance of the adaptive observers based on LOL model is evaluated against UKF based on a simplified drift-flux model by using measurements from the OLGA simulator. The adaptive observers are compared with each other in terms of rate of convergence and accuracy. Robustness of

the adaptive observers is investigated in case of errors in the reservoir and well parameters of the models.

This paper consists of the following sections: Section 2 describes the basic concept of the UBD process. The modeling section 3 presents a LOL and simplified drift-flux model based on mass and momentum balances for UBD operation and the reservoir model. Section 4 explains the Lyapunov-based adaptive observer and joint UKF methods for simultaneously estimating the states and model parameters from real-time measurements. Section 5, at the end the conclusion of the paper is presented.

2. Under balanced drilling

In drilling operations, the drilling fluid is pumped down the drill string and through the drill bit into the well (see Figure 1). The annulus is sealed with a rotating control device (RCD), and the drilling fluid exits through a controlled choke valve, allowing for faster and more precise control of the annular pressure. The drilling fluid carries cuttings from the drill bit to the surface.

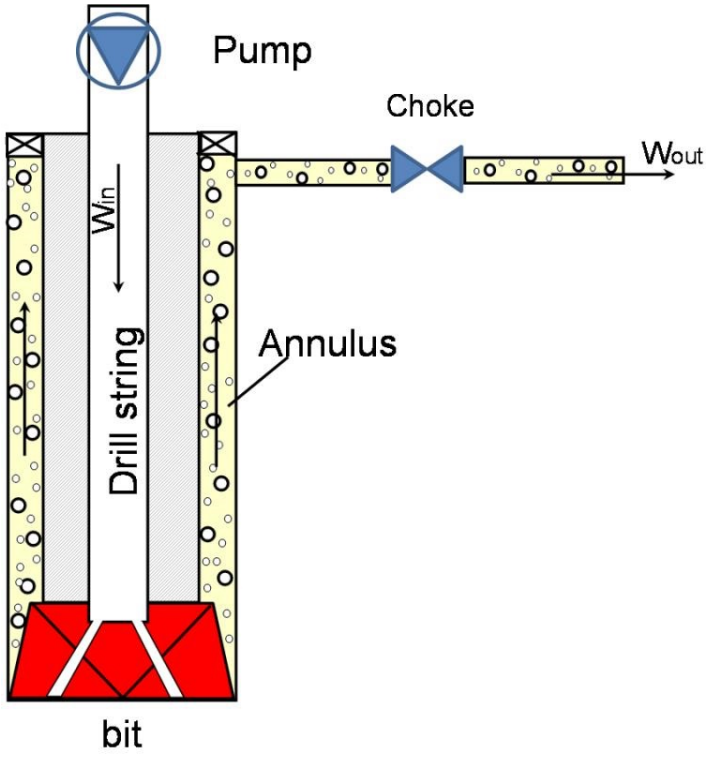

Figure 1: Schematic of an UBD system

In conventional (over-balanced) drilling, or managed pressure drilling (MPD), the pressure in the well is kept greater than the pressure of the reservoir to prevent influx from entering the well [22]. In UBD operations, on the other hand the pressure of the well is kept

below the pressure of the reservoir, allowing formation fluid flow into the well during the drilling operation.

Nitrogen unit, Rotating control devices (RCD), Chemical injection equipment, Surface separation equipment, choke and manifold system, geologic sampler, emergency shut-down system and Non-return valve (NRV) are the main surface equipments involved in normal UBD operations [23]. The pump flow rate, choke valve and density of the drilling fluid (mud) are the various inputs used to adjust the pressure in the well-bore. The choke valve is the most common input used to regulate the pressure in the annulus during MPD and UBD operations. Furthermore, real time knowledge of states and parameters of a dynamic model for the multi phase flow in the well is very useful in controllers, fault detection systems and safety applications in the well during petroleum exploration and production drilling. Some states of a dynamic model of multi phase flow in the well can not be measured directly or have a delay or low measurement frequency, and some parameters may be varied only during drilling. So, states and parameters of the dynamic model of multi phase flow in the well must be estimated.

3. Modeling

Due to the existence of multiphase flow (i.e. oil, gas, water, drilling fluid and cuttings) in the system, the modeling of the system is challenging. Multiphase flow can be modeled by a distributed model or a simplified LOL model. A distributed model is capable of describing the gas-liquid behavior along the annulus in the well. The simplified LOL model is based on some simplifying assumptions, and considers only the gas-liquid behavior at the drill bit and the choke system. The LOL model used in this paper is very similar to the two-phase flow model found in [11, 24]. In the simplified drift-flux model and the LOL model, the drilling fluid, oil, water, and rock cuttings are lumped into the liquid phase. Both models neglect the effects of cutting transport as one of their assumption.

3.1. Simplified drift-flux model

There are two common methods for modeling distributed multiphase flow in UBD operations. The most general and detailed method is called a two-fluid model. This method uses four partial differential equations (PDE's) for conservation of mass and momentum in each phase. The two-fluid model is difficult to solve both analytically or numerically, because the source terms reflecting interphase drag are stiff and this can lead to significant problems in the numerical computation [25]. Due to the complexity of the two-fluid model, the drift-flux model is derived by merging the momentum equations of both phases (gas/liquid) into one equation. Therefore, difficult phase interaction terms cancel out, and the missing information in the mixture momentum equation must be replaced by a slip equation which gives a relation between the flow velocities of the phases. The mechanistic models use different relations between the phase slip velocities and pressure loss terms for different flow patterns [9, 26]. These models need to predict flow patterns at each time step. In this paper, a simplified drift-flux model (DFM) is used. The simple DFM uses a specific empirical slip law, without flow-regime predictions, but which allows for transition between single and

two phase flows. The isothermal simple DFM formulation of the conservation of mass and momentum balance are given by [27]

$$\frac{\partial m}{\partial t} + \frac{\partial m v_l}{\partial x} = 0, \tag{1}$$

$$\frac{\partial n}{\partial t} + \frac{\partial n v_g}{\partial x} = 0, \tag{2}$$

$$\frac{\partial (m v_l + n v_g)}{\partial t} + \frac{\partial (P + m v_l^2 + n v_g^2)}{\partial x} = -(m+n) g \cos \Delta\theta - \frac{2 f (m+n) v_m |v_m|}{D}. \tag{3}$$

where the mass variables are defined as follows

$$m = \alpha_l \rho_l, \qquad\qquad n = \alpha_g \rho_g$$

where $k = l, g$ denoting iquid and gas, respectively, ρ_k is the phase density, and α_k is the volume fraction satisfying

$$\alpha_l + \alpha_g = 1. \tag{4}$$

Further v_k denotes the velocities, and P the pressure. All of these variables are functions of time and space. We denote $t \geq 0$ the time variable, and $x \in [0, L]$ the space variable, corresponding to a curvilinear abscissa with $x = 0$ corresponding to the bottom hole and $x = L$ to the outlet choke position. In the momentum equation (3), the term $(m+n)g \cos \Delta\theta$ represents the gravitational source term, g is the gravitational constant and $\Delta\theta$ is the mean angle between gravity and the positive flow direction of the well, while $-\frac{2f(m+n)v_m|v_m|}{D}$ accounts for frictional losses. The closure relations, boundary conditions and discretization schemes for this model can be found in [27].

3.2. LOL model

The so-called low-order lumped (LOL) model is perhaps the simplest method for modeling multiphase flow in UBD. A LOL model is suitable for conventional model-based control design methods and can be used for prediction and estimation in an observer and controller algorithms. The most important simplifying assumptions of the LOL model are listed as below:[11, 28]

- Ideal gas behavior
- Simplified choke model for gas, mud and liquid leaving the annulus
- No mass transfer between gas and liquid
- Isothermal condition and constant system temperature
- Constant liquid density with respect to pressure and temperature
- Uniform flow pattern along the whole drill string and annulus

The simplified LOL model equations for mass of gas and liquid in the annulus are derived from mass and momentum balances as follows [16]

$$\dot{m}_g = w_{g,d} + w_{g,res}(m_g, m_l) - \frac{m_g}{m_g + m_l} w_{out}(m_g, m_l) \tag{5}$$

$$\dot{m}_l = w_{l,d} + w_{l,res}(m_g, m_l) - \frac{m_l}{m_g + m_l} w_{out}(m_g, m_l) \tag{6}$$

where m_g and m_l are the total mass of gas and liquid, respectively. The liquid phase is assumed incompressible, and ρ_l is the liquid mass density. The gas phase is compressible and occupies the volume left free by the liquid phase. $w_{g,d}$ and $w_{l,d}$ are the mass flow rates of gas and liquid from the drill string, and $w_{g,res}$ and $w_{l,res}$ are the mass flow rates of gas and liquid from the reservoir. The total mass outflow rate is

$$w_{out} = K_c Z \sqrt{\frac{m_g + m_l}{V_a}} \sqrt{p_c - p_{c0}} \tag{7}$$

where K_c is the choke constant, and Z is the control signal to the choke opening, taking its values on the interval $(0, 1]$. The total volume of the annulus is denoted by V_a, and p_{c0} is the constant downstream choke pressure (atmospheric). The choke pressure is denoted by p_c, and derived from ideal gas equation

$$p_c = \frac{RT}{M_{gas}} \frac{m_g}{V_a - \frac{m_l}{\rho_l}} \tag{8}$$

where R is the gas constant, T is the average temperature of the gas, and M_{gas} is the molecular weight of the gas. The bottom-hole pressure is given by the following equation

$$p_{bh} = p_c + \frac{(m_g + m_l) g \cos(\Delta\theta)}{A} + \Delta p_f \tag{9}$$

where A is the cross sectional area of the annulus, Δp_f is the friction pressure loss in the well

$$\Delta p_f = K_f (w_{g,d} + w_{l,d})^2 \tag{10}$$

and K_f is the friction factor.

3.3. Reservoir flow

The mass flow from the reservoir into the well for each phase is modeled by a linear relation

$$w_{g,res} = \begin{cases} K_g(p_{res} - p_{bh}), & \text{if } p_{res} > p_{bh} \\ 0, & \text{otherwise.} \end{cases} \tag{11}$$

$$w_{l,res} = \begin{cases} K_l(p_{res} - p_{bh}), & \text{if } p_{res} > p_{bh} \\ 0, & \text{otherwise.} \end{cases} \tag{12}$$

where p_{res} is the known pore pressure in the reservoir, and K_g and K_l are the production constants of gas and liquid from the reservoir into the well, respectively. Reservoir parameters could be evaluated by seismic data and other geological data from core sample analysis. Still, local variations of reservoir parameters such as the production constants of gas and liquid may be revealed only during drilling. So, it is valuable to estimate the partial variations of some of the reservoir parameters while drilling is performed ([8]).

4. Estimation Algorithm

In this section, first a Lyapunov-based adaptive observer to estimate states and parameters in UBD operation for the LOL model is derived. Then, the joint unscented Kalman filter is presented for both the distributed and LOL models. The measurements and inputs of models are summarized in Table 1. We assume the pore pressure p_{res} is known, and the production constant of gas (K_g) and liquid (K_l) from the reservoir into the well are unknown and must be estimated. We will later mention why p_{res} can be assumed known by considering offline estimation and study the sensitivity to errors in p_{res}. K_g and K_l are named by θ_1 and θ_2, respectively, for notational purposes.

Table 1: Measurements and Inputs

Variables	Measurement/Input
Choke pressure (p_c)	Measurement
Bottom-hole pressure (p_{bh})	Measurement
Drill string mass flow rate of gas ($w_{g,d}$)	Input
Drill string mass flow rate of liquid ($w_{l,d}$)	Input
Choke opening (Z)	Input

The friction factor (k_f) and choke constant (k_c) of the model are assumed known. These parameters could be estimated offline by using separation flow rates and topside data. Other parameters that are used in this paper such as density, temperature and well volume can typically come from well data.

4.1. Lyapunov-based adaptive observer

A full-order state observer for the system (5)-(6) is

$$\dot{\hat{m}}_g = w_{g,d} + \hat{w}_{g,res}(\hat{\theta}_1) - \frac{\hat{m}_g}{\hat{m}_g + \hat{m}_l}\hat{w}_{out}(\hat{m}_g, \hat{m}_l) + k_1(p_{bh} - \hat{p}_{bh}) \tag{13}$$

$$\dot{\hat{m}}_l = w_{l,d} + \hat{w}_{l,res}(\hat{\theta}_2) - \frac{\hat{m}_l}{\hat{m}_g + \hat{m}_l}\hat{w}_{out}(\hat{m}_g, \hat{m}_l) + k_2(p_{bh} - \hat{p}_{bh}) \tag{14}$$

where

$$\hat{w}_{g,res} = \hat{\theta}_1(p_{res} - p_{bh}) \tag{15}$$

$$\hat{w}_{l,res} = \hat{\theta}_2(p_{res} - p_{bh}) \tag{16}$$

$$\hat{w}_{out} = K_c Z \sqrt{\frac{\hat{m}_g + \hat{m}_l}{V_a}} \sqrt{p_c - p_{c0}} \tag{17}$$

$$\hat{p}_{bh} = p_c + \frac{(\hat{m}_g + \hat{m}_l) g \cos(\Delta\theta)}{A} + \Delta p_f \tag{18}$$

Note that the observer gains are chosen equal ($k_1 = k_2$) since it is based on Lyapunov theorem. However, in practice it might be possible to choose different gains based on tuning since Lyapunov theorem is conservative. $\frac{k_1}{A} = l_1$, has to be chosen sufficiently large positive. $\hat{m}_g$ and $\hat{m}_l$ are estimates of states m_g and m_l. Define the state estimation errors $e_1 = m_g - \hat{m}_g$ and $e_2 = m_l - \hat{m}_l$, and let $\hat{\theta}_1$ and $\hat{\theta}_2$ be estimates of parameters $\theta_1 = K_g$ and $\theta_2 = K_l$. Next, we define parameter estimation laws

$$\dot{\hat{\theta}}_1 = q_1 (p_{res} - p_{bh}) e_1 \tag{19}$$

$$\dot{\hat{\theta}}_2 = q_2 (p_{res} - p_{bh}) e_2 \tag{20}$$

where the gains q_1 and q_2 are positive tuning parameters that specify trade-offs in the observer design. Choosing larger gains results in faster convergence but large overshoot and undershoot in estimation, or sometimes instability. Choosing smaller gains results in slower convergence and small overshoot and undershoot, or sometimes without any overshoot in estimation. Since the total mass of gas and liquid in the well could not be measured directly, they are computed by solving a series of nonlinear algebraic equations (8)-(9) using measurements of the choke and the bottom-hole pressures.

$$m_l^c = \frac{1}{1 - \frac{p_c M_{gas}}{RT\rho_l}} \left(\frac{(p_{bh} - p_c - \Delta p_f) A}{g \cos(\Delta\theta)} - \frac{p_c M_{gas} V_a}{RT} \right) \tag{21}$$

$$m_g^c = \frac{p_c M_{gas} (V_a - \frac{m_l^c}{\rho_l})}{RT} \tag{22}$$

The adaptation laws (19)-(20) can be implemented by using $e_1 = m_g^c - \hat{m}_g$ and $e_2 = m_l^c - \hat{m}_l$. The error dynamics can be written as follows

$$\dot{e_1} = (\theta_1 - \hat{\theta}_1)(p_{res} - p_{bh}) - (\frac{m_g}{m_g + m_l} w_{out} - \frac{\hat{m_g}}{\hat{m}_g + \hat{m}_l} \hat{w}_{out}) - l_1 g \cos(\Delta\theta)(e_1 + e_2) \tag{23}$$

$$\dot{e_2} = (\theta_2 - \hat{\theta}_2)(p_{res} - p_{bh}) - (\frac{m_l}{m_g + m_l} w_{out} - \frac{\hat{m_l}}{\hat{m}_g + \hat{m}_l} \hat{w}_{out}) - l_1 g \cos(\Delta\theta)(e_1 + e_2) \tag{24}$$

Let $\tilde{\theta}_1 = \theta_1 - \hat{\theta}_1$, $\tilde{\theta}_2 = \theta_2 - \hat{\theta}_2$, and the Lyapunov function candidate for the adaptive observer design be defined as

$$V(e, \tilde{\theta}) = \frac{1}{2} (e_1^2 + e_2^2 + q_1^{-1} \tilde{\theta}_1^2 + q_2^{-1} \tilde{\theta}_2^2) \tag{25}$$

It is easy to check that $V(e, \tilde{\theta})$ is positive definite, and we continue to analyze if it can be made decrescent. From (23) and (24), the time derivative of $V(e, \tilde{\theta})$ along the trajectory of

the error dynamics is

$$\begin{aligned}\dot{V}(e,\tilde{\theta}) = &- l_1 g\cos(\Delta\theta)(e_1+e_2)^2 - \frac{e_1^2 w_{out}}{m_g+m_l} + \tilde{\theta}_1\ [(p_{res}-p_{bh})e_1 + q_1^{-1}\dot{\tilde{\theta}}_1] \\ &+ \tilde{\theta}_2\ [(p_{res}-p_{bh})e_2 + q_2^{-1}\dot{\tilde{\theta}}_2] - \frac{\hat{m}_l e_2(w_{out}-\hat{w_{out}})}{\hat{m}_g+\hat{m}_l} - \frac{e_2^2 w_{out}}{m_g+m_l} - \frac{\hat{m}_g e_1(w_{out}-\hat{w_{out}})}{\hat{m}_g+\hat{m}_l} \\ &+ \frac{\hat{m}_l e_2(e_1+e_2)w_{out}}{(m_g+m_l)(\hat{m}_g+\hat{m}_l)} + \frac{\hat{m}_g e_1(e_1+e_2)w_{out}}{(m_g+m_l)(\hat{m}_g+\hat{m}_l)} \end{aligned} \tag{26}$$

The detail calculations of the derivative of the Lyapunov function is presented in [17] :

$$\begin{aligned}\implies \dot{V}(e,\tilde{\theta}) < &- l_1 g\cos(\Delta\theta)(e_1^2+e_2^2) - \frac{w_{out}(\ e_1^2+e_2^2)}{m_g+m_l+\sqrt{m_g+m_l}\sqrt{\hat{m}_g+\hat{m}_l}} \\ &- e_1 e_2(\ 2l_1 g\cos(\Delta\theta) - \frac{w_{out}(\frac{\sqrt{\hat{m}_g+\hat{m}_l}}{\sqrt{m_g+m_l}})}{m_g+m_l+\sqrt{m_g+m_l}\sqrt{\hat{m}_g+\hat{m}_l}})\end{aligned} \tag{27}$$

By choosing l_1 sufficiently large, then

$$0 \le \left(\ 2l_1 g\cos(\Delta\theta) - \frac{w_{out}(\frac{\sqrt{\hat{m}_g+\hat{m}_l}}{\sqrt{m_g+m_l}})}{m_g+m_l+\sqrt{m_g+m_l}\sqrt{\hat{m}_g+\hat{m}_l}}\right) < 2l_1 g\cos(\Delta\theta) \tag{28}$$

The lower bound of l_1 is

$$\begin{aligned}&2l_1 g\cos(\Delta\theta) - (\frac{w_{out}}{m_g+m_l})\left(\frac{\sqrt{\hat{m}_g+\hat{m}_l}}{\sqrt{m_g+m_l}+\sqrt{\hat{m}_g+\hat{m}_l}}\right) \ge 0 \\ &\left(\frac{\sqrt{\hat{m}_g+\hat{m}_l}}{\sqrt{m_g+m_l}+\sqrt{\hat{m}_g+\hat{m}_l}}\right) < 1 \quad , (\frac{w_{out}}{m_g+m_l}) < \gamma\end{aligned} \tag{29}$$

$$\implies\ l_1 > \frac{\gamma}{2g\cos(\Delta\theta)} \tag{30}$$

In real drilling problem we usually have ($\gamma \ll 1$), therefore the lower bound of l_1 is small, and this gives

$$\begin{aligned}\dot{V}(e,\tilde{\theta}) < &-l_1 g\cos(\Delta\theta)(e_1^2+e_2^2) + 2l_1 g\cos(\Delta\theta)|e_1||e_2| \\ &- \frac{w_{out}(\ e_1^2+e_2^2)}{m_g+m_l+\sqrt{m_g+m_l}\sqrt{\hat{m}_g+\hat{m}_l}}\end{aligned} \tag{31}$$

By using Young's inequality $2|e_1||e_2| \le e_1^2+e_2^2$,

$$\dot{V}(e,\tilde{\theta}) < -\frac{w_{out}(\ e_1^2+e_2^2)}{m_g+m_l+\sqrt{m_g+m_l}\sqrt{\hat{m}_g+\hat{m}_l}} \le 0 \tag{32}$$

which implies that all signals $e_1, e_2, \tilde{\theta}_1, \tilde{\theta}_2$ are bounded. From (23),(24) and $e_1, e_2, \tilde{\theta}_1, \tilde{\theta}_2 \in \mathcal{L}_\infty$, $\dot{e_1}, \dot{e_2}$ are bounded. It follows by using Barbalat's lemma that e_1, e_2 converge to zero. Since there are no couplings between the parameter estimates based on equations (19)-(20), the convergence of the two parameter estimates can be analyzed independently as scalars. The adaptation laws can be written as follows:

$$\begin{aligned} \dot{\hat{\theta}}_i &= q_i \phi e_i && i = 1, 2 \\ \phi &= (p_{res} - p_{bh}) && (scalar) \end{aligned} \tag{33}$$

Based on the persistency excitation theorem, $\lim_{t\to\infty} \hat{\theta} = \theta^*$ if and only if there exists some $\alpha, T > 0$ such that, for any $t > 0$, the following inequality is satisfied ([19]):

$$\int_t^{t+T} \phi(\tau)\phi^T(\tau)\, \mathrm{d}\tau \geq \alpha > 0, \quad \forall t \geq t_0 \tag{34}$$

So, the persistency excitation theorem can be applied independently as scalar for each parameter estimate as follow:

$$\int_t^{t+T} \phi(\tau)\phi^T(\tau)\, \mathrm{d}\tau = \int_t^{t+T} (p_{res}(\tau) - p_{bh}(\tau))^2\, \mathrm{d}\tau \geq \alpha > 0, \quad \forall t \geq t_0 \tag{35}$$

Thus according to theorem 4.9 in [29], the adaptive observer system is globally asymptotically stable if the persistency excitation condition is satisfied. A necessary and sufficient condition is that there must be flow from the reservoir to satisfy persistence exciting condition, since it is equivalent with $p_{res} \neq p_{bh}$.

4.2. Joint Unscented Kalman Filter

The Kalman filter using linearization to estimate both the state and parameter vectors of the system is usually known as an augmented Kalman filter. The UKF technique has been developed to work with non-linear systems without using a Jacobian-based linearization of the model ([30, 31]). The UKF estimates the mean and covariance matrix of the estimation error with a minimal set of sample points (called sigma points) around the mean by using a deterministic sampling approach known as the unscented transform. The nonlinear model is applied to propagate uncertainty of sigma points instead of using a linearization of the model. So, this method does not need to calculate the explicit Jacobian or Hessian. More details can be found in ([31, 20]).

The augmented state vector is defined by $x^a = [X, \theta]$ where X is the state of the model. The discrete time state-space equations for the the augmented state vector at time instant k is written as:

$$\begin{bmatrix} X_k \\ \theta_k \end{bmatrix} = \begin{bmatrix} f(X_{k-1}, \theta_{k-1}) \\ \theta_{k-1} \end{bmatrix} + q_k = f^a(X_{k-1}, \theta_{k-1}) + q_k \tag{36}$$

where $q_k \sim N(0, Q_k)$ is the zero mean Gaussian process noise (model error). Here, we apply the UKF to both the LOL and DFM. When using the DFM, the number of states that must

be estimated by the joint UKF is equal to three times of the number of spatial discretization cells in the DFM. The discrete measurements of the system can be modeled as follows:

$$y_k = h(X_k) + r_k \tag{37}$$

$$h(X_k) = [p_c, p_{bh}]^T \tag{38}$$

where $r_k \sim N(0, R_k)$ is the zero mean Gaussian measurement noise.

5. Simulation Results

The parameter values for the simulated well and reservoir are summarized in Table 2, and used in the OLGA simulator. The measurements have been synthetically generated by using the OLGA dynamic multiphase flow simulator. The OLGA simulator uses the same model for the mass flow from the reservoir into the well as in equations (11)-(12).

Table 2: Parameter Values for Well and Reservoir

Name	DFM	Unit
Reservoir pressure (p_{res})	279	bar
Collapse pressure (p_{coll})	155	bar
Well total length (L_{tot})	2530	m
Drill string outer diameter (D_d)	0.1206	m
Annulus inner diameter (D_a)	0.1524	m
Liquid flow rate ($w_{l,d}$)	13.33	kg/s
Gas flow rate ($w_{g,d}$)	0	kg/s
Liquid density (ρ_L)	1000	kg/m^3
Production constant of liquid (K_L)	0.1	kg/s/bar
Production constant of liquid (K_g)	0.05	kg/s/bar
Gas average temperature (T)	285.15	K
Average angle ($\Delta\theta$)	0	rad
Choke constant (K_c)	0.0057	m^2

A discretization of the time and space variables is required for using numerical methods. The PDE of the drift-flux model are discretized by using a finite volumes method for the joint UKF based on DFM. where 6 cells were used for the spatial discretization. A measurement sampling period of 10 seconds were used and the model was run with time steps of 10 seconds. The parameter values for the nonlinear adaptive observer and UKF for both models are summarized in Table 3.

The initial values for the estimated and real parameters are as follows:

$$K_g = 0.05, \quad K_l = 0.1, \quad \hat{K_g} = 0.07, \quad \hat{K_l} = 0.13$$

Table 3: Parameter Values for Model and Estimators

Parameter	Value	Parameter	Value
q_1	2.5×10^{-13}	k_1	4×10^{-9}
q_2	5×10^{-14}	L	4
κ_{LOL}	0	κ_{DFM}	0
α_{LOL}	0.00001	α_{DFM}	0.00001
β_{LOL}	2	β_{DFM}	2

The case study that is used in this paper considers UBD operation of a vertical well drilled into an oil and gas reservoir. Two scenarios are simulated. In first scenario, first drilling in a steady-state condition is initiated with the choke opening of 12 %. After 1 hour, there is a linear decrease in the choke opening from 12 % to 8 % for 1 hour. After 4 hours, there is a linear increase in the choke opening from 8 % to 12 % for 1 hour. After 7 hours, there is a linear and sharp increase in the production constant of gas from 0.05 kg/s/bar to 0.07 kg/s/bar (change of reservoir height). Choke opening in this simulation is illustrated in Figure 2.

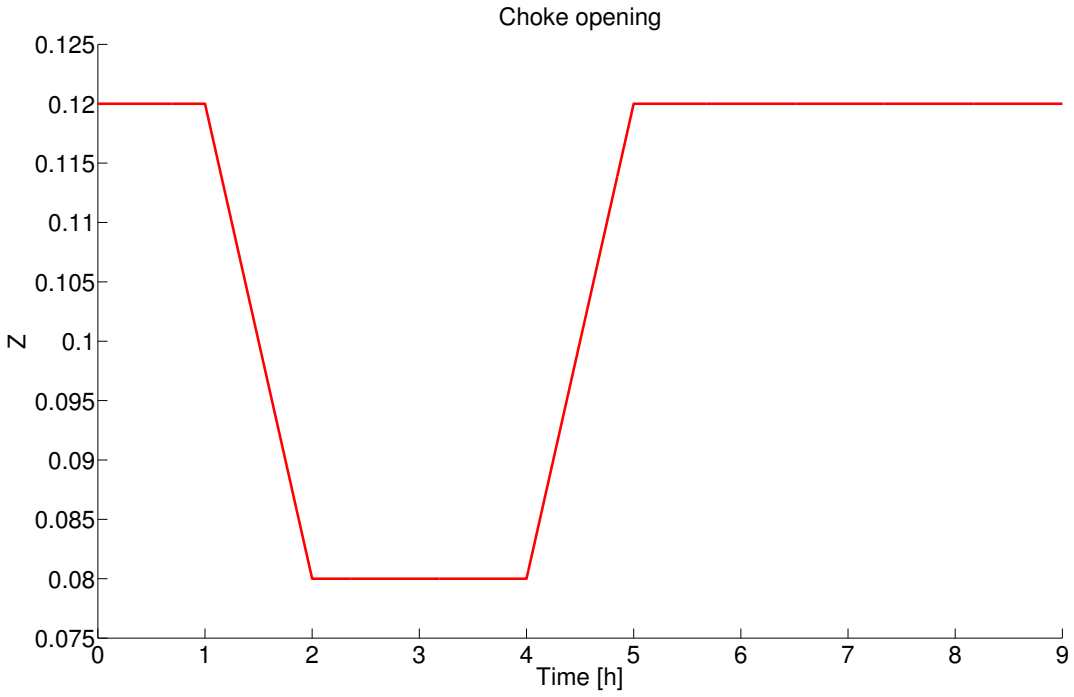

Figure 2: Choke opening

The parameter covariance matrix of UKF used for both models and scenarios is

$$Q = diag[8 * 10^{-9}, 2 * 10^{-8}]$$

Choosing the process noise covariance matrix in the UKF (Q_k) specify trade-offs in the UKF design. Choosing larger process noise in the UKF (Q_k) leads to faster track of data and convergence but typically more uncertainty in the estimation. Choosing smaller process noise in the UKF (Q_k) leads to slower track of data and convergence but typically less uncertainty in the estimation. The choke and the bottom-hole pressure measurements are corrupted by zero mean additive white noise with the following covariance matrix

$$R = \begin{bmatrix} 0.9 * 0.4^2 & 0 \\ 0 & 0.9 * 0.2^2 \end{bmatrix} (bar^2)$$

In order to estimation the reservoir pressure offline, consider Li's method. Figure 3 shows the best-fit regression line between the three points of estimation based on two characteristics of the well, total gas flow rate from the reservoir and the bottom hole pressure. The time of testing points are chosen 1.5, 3 and 6 hours. The offline estimation of reservoir pressure is 278.8, calculated by using Li's method. This estimation is very close to the actual value of 279 bar obtained from OLGA simulator. The total flow rate from the reservoir can be estimated by the Lyapunov-based adaptive observer in section 4 by changing adaptation laws for estimation of the total gas flow rate from the reservoir instead of the production constants.

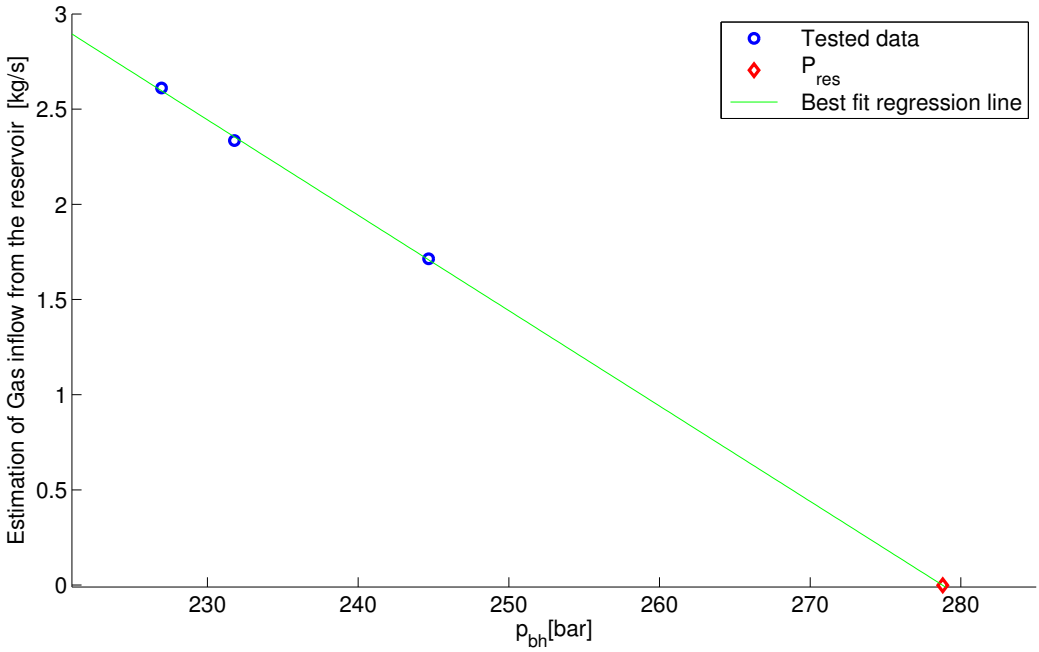

Figure 3: Estimation of total gas flow rate from the reservoir versus the bottom hole pressure and the best-fit regression line.

The estimation of the production constants of gas and liquid from the reservoir into the well are shown in Figures 4 and 5, respectively. The estimates of all algorithms are

converging quite fast, about 0.5 hour. UKF based on LOL model produces less accurate results than the other methods for estimation of the production constant of gas from the reservoir into the well during transient time. The results is shown that reasonable performance of the estimation algorithms to detect and track changing at production constant of gas. The Lyapunov-based adaptive observer has better performance than the other methods for estimation of the production constants of gas and liquid from the reservoir into the well when the production constant of gas is increased from 0.05 kg/s/bar to 0.07 kg/s/bar. In DFM, it is expected that estimation of the slip parameters can improve accuracy of the production parameters estimation [14]. Therefore, errors in slip parameters might cause a bias in the estimation of the production parameters with UKF based on DFM when the reservoir parameters change.

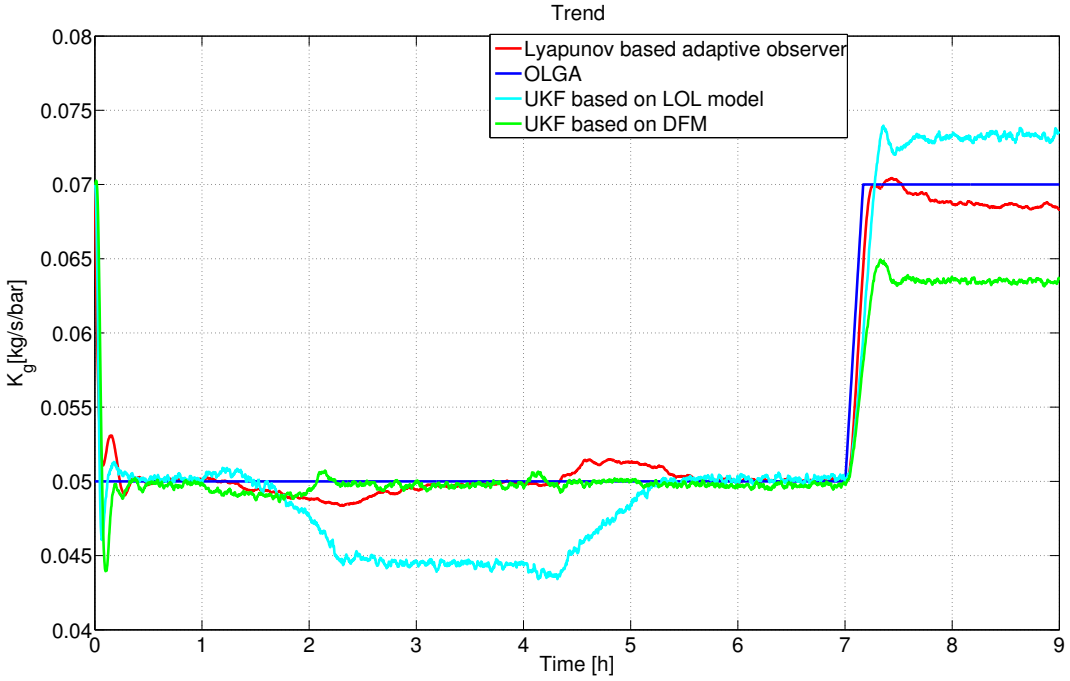

Figure 4: Actual value and estimated production constant of gas

The measured and estimated bottom-hole pressure and choke pressure at the wellhead are illustrated in Figures 6 and 7, respectively. The only error measurement that was injected to the nonlinear Lyapunov-based adaptive observer is bottom hole pressure. Since the choke pressure in LOL model during transient time has an error, estimation of choke pressure with the nonlinear Lyapunov-based adaptive observer has a bias during transient time and estimation of bottom hole pressure with UKF has a bias during transient time. Since the LOL model is a much simpler model than the distributed model, it has some mismatch with OLGA simulator. So, this mismatch influences the estimation of parameters and states. The measurement covariance of the UKF determines the priority of measurements for the UKF. The Lyapunov adaptive observer tries to reduce errors of states and parameters by injecting

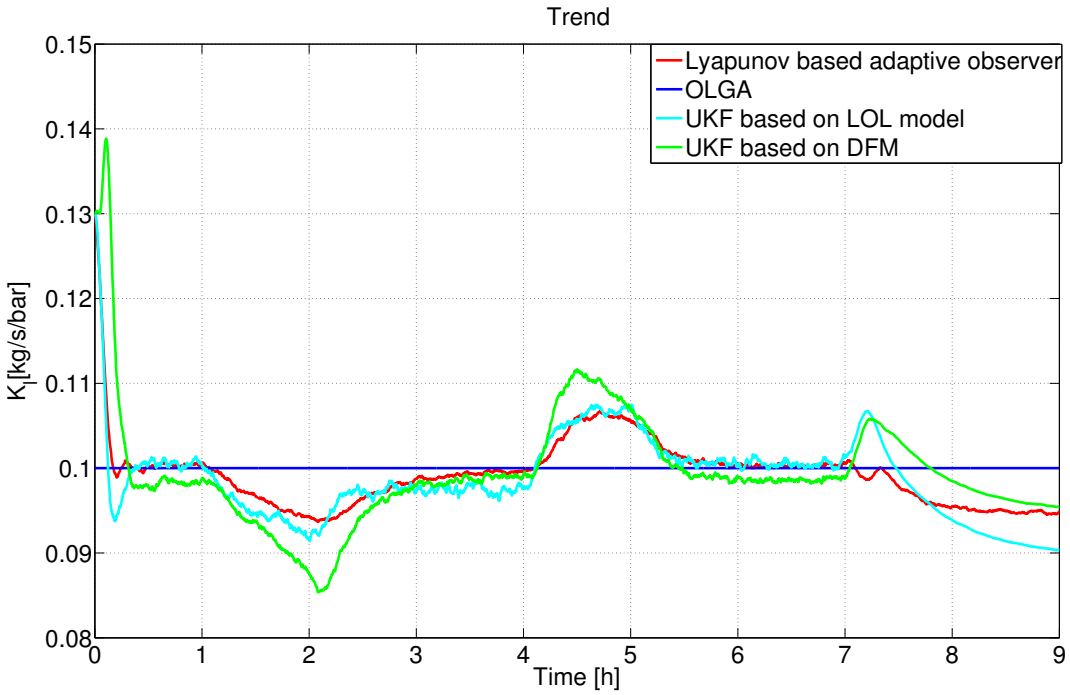

Figure 5: Actual value and estimated production constant of liquid

the error between estimation and measurement of bottom hole pressure (the last terms in Equations (13) and (14)). The bottom hole pressure and the choke pressure are correlated with each other with the mass and momentum balances. So, the error between estimation and measurement of choke pressure is indirectly affected by the Lyapunov adaptive observer. But, the error between estimation and measurement of bottom hole pressure is affected directly by the Lyapunov adaptive observer. Simulation time of the adaptive observers based on LOL model executes at least 100 times faster than joint UKF based on DFM.

In this paper, performance of the adaptive observers is evaluated through the root mean square error (RMSE) metric for the parameters K_g and K_l . The RMSE metric for the Lyapunov-based adaptive observer and UKF for both models during the whole estimation period and after initial transient ($t \geq 0.5hour$) are summarized in Table 4.

Table 4: RMSE metric

Method	Whole estimation period		After initial transient	
	K_g	K_l	K_g	K_l
Lyapunov-based adaptive observer	1.4×10^{-3}	4.0×10^{-3}	1.1×10^{-3}	3.3×10^{-3}
UKF based on LOL model	3.6×10^{-3}	5.0×10^{-3}	3.4×10^{-3}	4.5×10^{-3}
UKF based on DFM	3.5×10^{-3}	6.8×10^{-3}	3.3×10^{-3}	5.2×10^{-3}

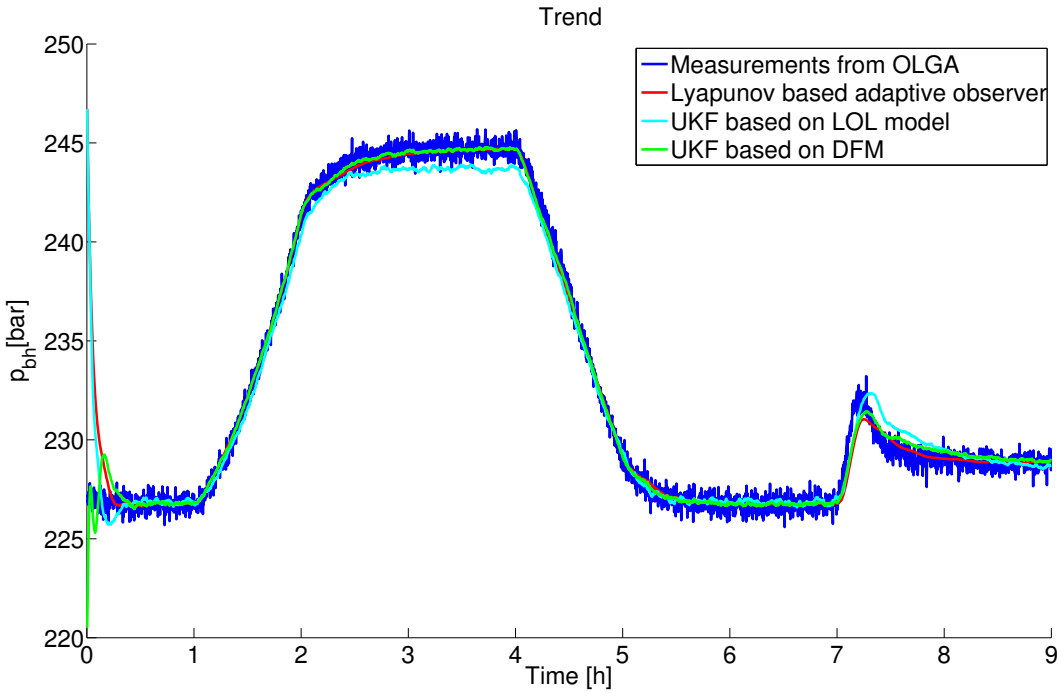

Figure 6: Measured and estimated bottom-hole pressure

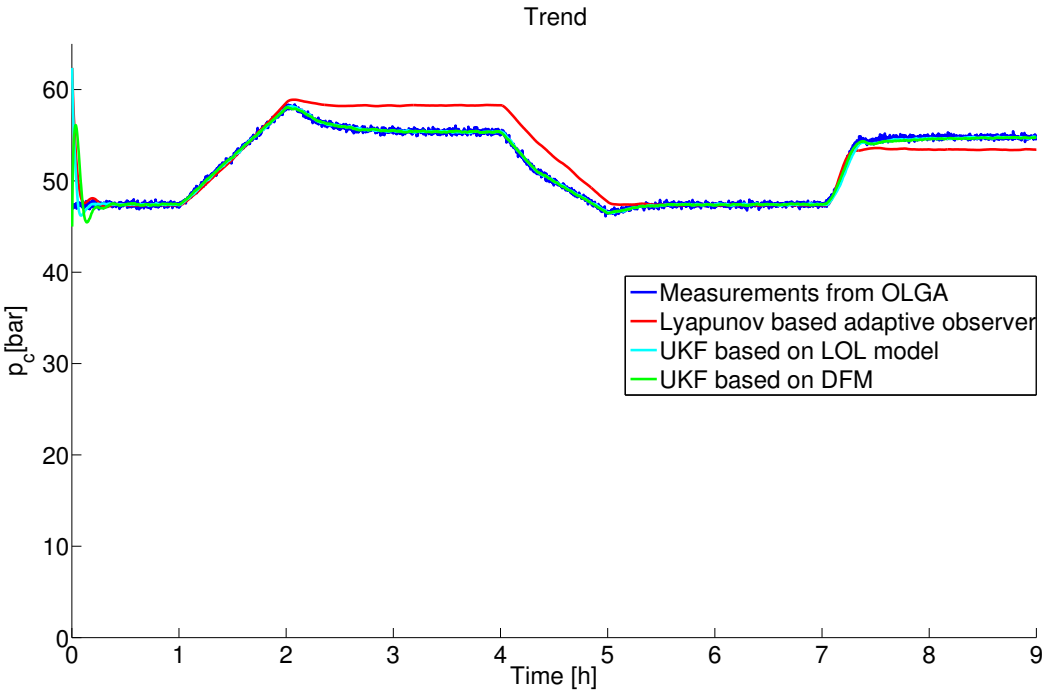

Figure 7: Measured and estimated choke pressure

According to the RMSE metric Table 4, the Lyapunov-based adaptive observer has better performance than the other methods for estimation of the production constants of gas and liquid from the reservoir into the well. Robustness of the adaptive observers is tested in case of errors in the reservoir pore pressure and liquid density. The RMSE metric for the adaptive observers in case of 1% error on the reservoir pore pressure, and 10% error on the liquid density, are summarized in Table 5 and 6, respectively.

Table 5: RMSE metric in case of error in the reservoir pressure value

Method	K_g	K_l	p_{res} true	p_{res} model
Lyapunov-based adaptive observer	4×10^{-3}	8×10^{-3}	279	282
UKF based on LOL model	5.7×10^{-3}	9×10^{-3}	279	282
UKF based on DFM	5.9×10^{-3}	9.9×10^{-3}	279	282

Table 6: RMSE metric in case of error in the liquid density value

Method	K_g	K_l	ρ_L true	ρ_L model
Lyapunov-based adaptive observer	2.6×10^{-3}	5.2×10^{-3}	1000	1100
UKF based on LOL model	3.4×10^{-3}	6.4×10^{-3}	1000	1100
UKF based on DFM	3.6×10^{-3}	6.9×10^{-3}	1000	1100

Since the reservoir pore pressure has a direct effect on the mass flow rates from the reservoir into the well, small inaccuracies in the reservoir pore pressure have a significant effect on the estimation of production constants. Therefor these methods are very sensitive to errors in the reservoir pore pressure value. Based on Table 4 and 6,the adaptive observers based on LOL model are more sensitive to errors in the liquid density value than UKF based on DFM.

The second scenario in this case study is as follows, first the drilling in a steady-state condition is initiated with the choke opening of 10 %, then at t = 1 hour and 35 min the main pump is shut off to perform a connection procedure, and the choke is closed to 6 %. The rotation of the drill string and the circulation of fluids are stopped for 15 mins. Next after making the first pipe connection at t = 1 hour and 50 min the main pump and rotation of the drill string are restarted. After 1 hour and 45 min (i.e. 3 hour and 35 min), the choke is closed to 5 %, and the second pipe connection procedure is started, and is completed after 15 mins. Then the choke is opened to 10 % at t= 3 hours and 50 min. The measured bottom-hole pressure (p_{bh}), choke pressure (p_c), choke opening (Z), and mass flow rate of liquid from the drill string ($w_{l,d}$) is illustrated in Figure 8.

The parameter values for the nonlinear adaptive observer and UKF for both models for pipe connection scenario are the same as in the previous scenario. The initial values for the

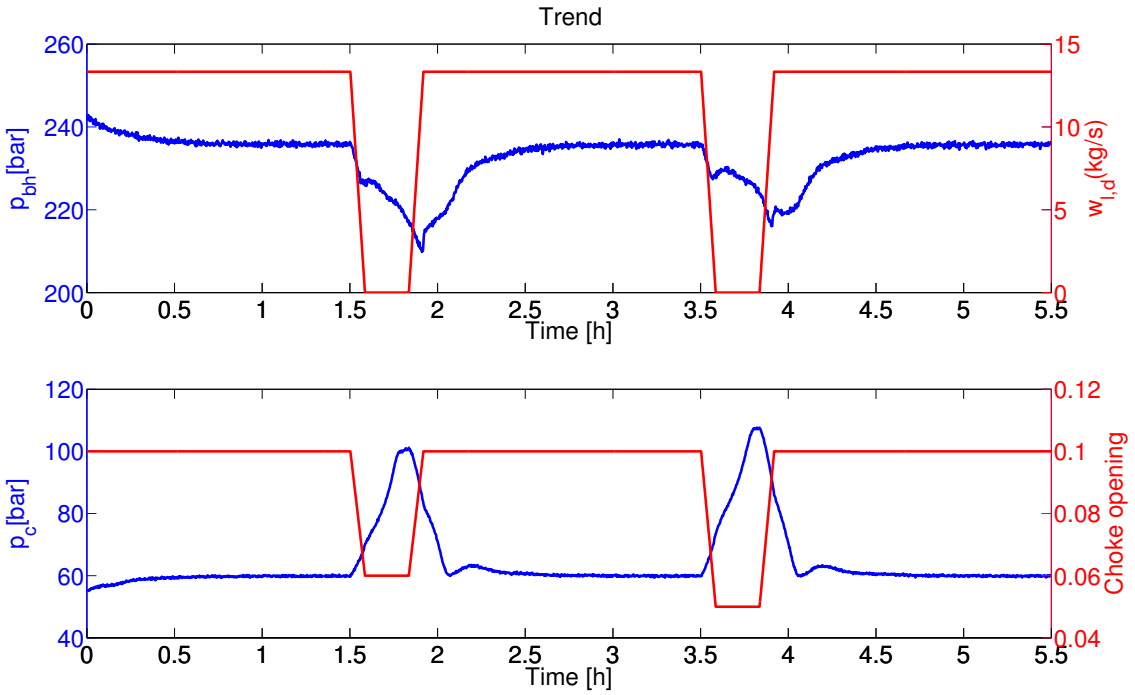

Figure 8: Measured bottom-hole pressure, choke pressure, choke opening, and mass flow rate of liquid from the drill string for pipe connection scenario

estimated and real parameters are as follows:

$$K_g = 0.07, \quad K_l = 0.1, \quad \hat{K}_g = 0.091, \quad \hat{K}_l = 0.13$$

The estimation of the production constants of gas and liquid from the reservoir into the well are shown in Figures 9 and 10, respectively. These parameters are identified with reasonable accuracy by all estimators. In estimation of production constant of liquid from the reservoir into the well, the Lyapunov-based adaptive observer has better performance than the other methods. Since the model is significantly less accurate during the pipe connection, we need to prevent that the PI estimates drift away. Hence, the gains value (q_1 and q_2) for the Lyapunov-based adaptive observer and the parameter covariance of UKF for both models are 1000 times smaller than the nominal value during the pipe connection. For the same reason, the measurement covariance of UKF for both models are 1000 times larger than the nominal value during the pipe connection.

The measured and estimated bottom-hole pressure and choke pressure at the wellhead for pipe connection scenario are illustrated in Figures 11 and 12, respectively. This results show that the adaptive observers have errors in the estimation of the bottom hole and choke pressure during pipe connection because the model is less accurate during pipe connection. Since the bottom hole and choke pressure are measured, errors of the bottom hole and choke pressure are not the main concern in this situation, since the purpose is estimation of production parameters. Nygaard et al. studied that some parameters of the model such

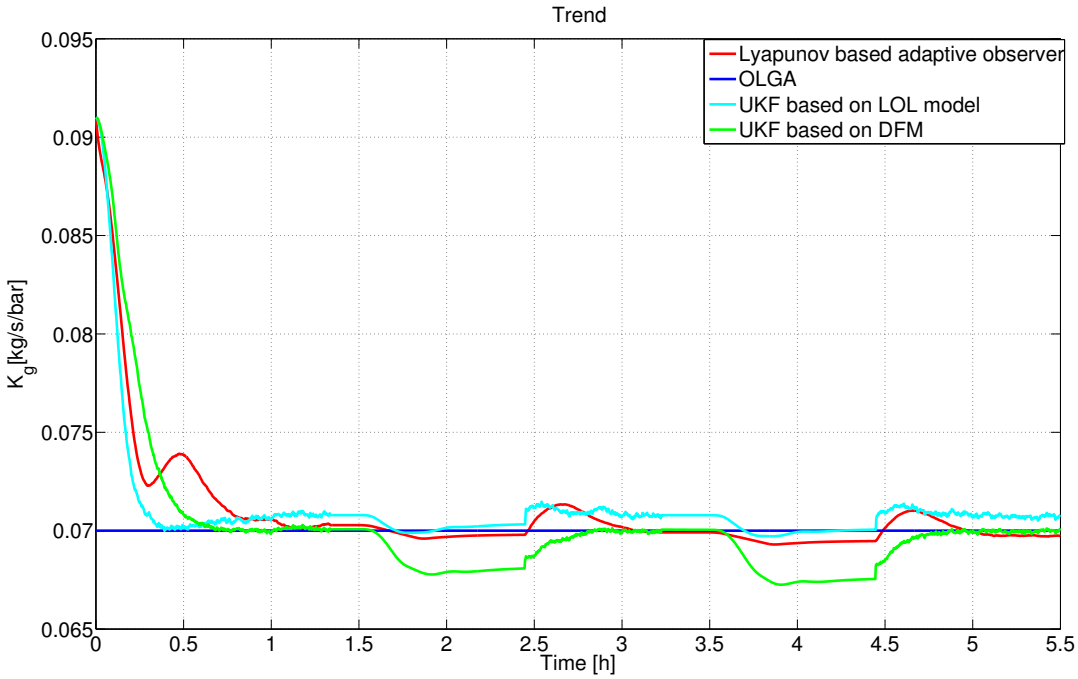

Figure 9: Actual value and estimated production constant of gas for pipe connection scenario

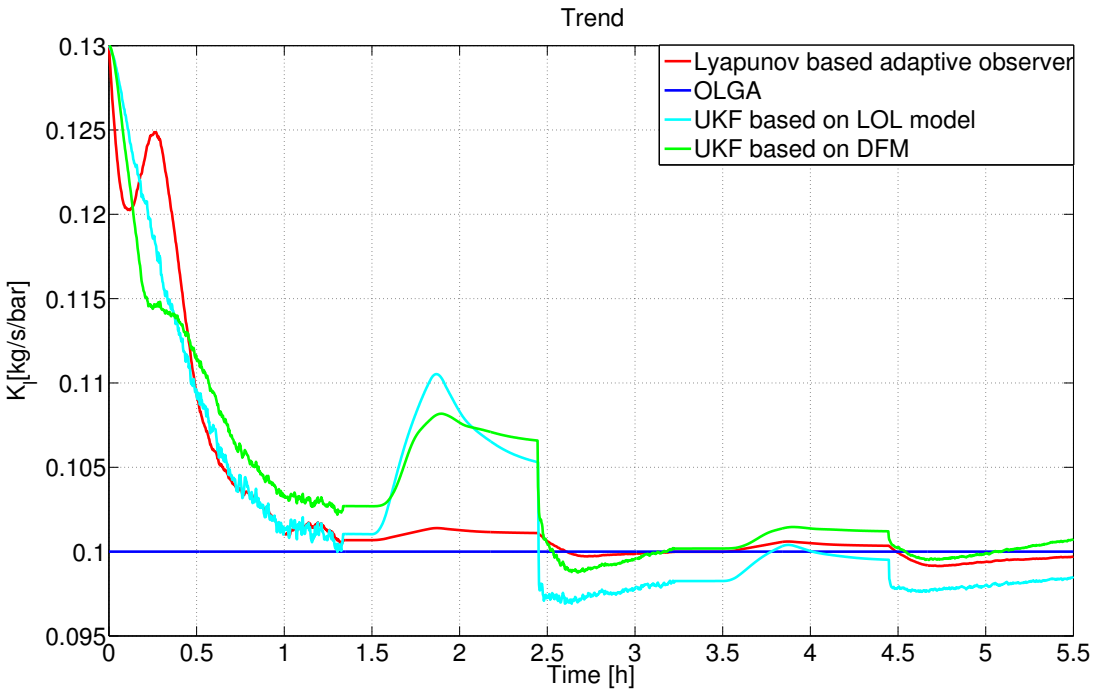

Figure 10: Actual value and estimated production constant of liquid for pipe connection scenario

as friction factor varies during pipe connection [10]. Since we assumed these parameters are constant, this introduces some errors to the model during pipe connection.

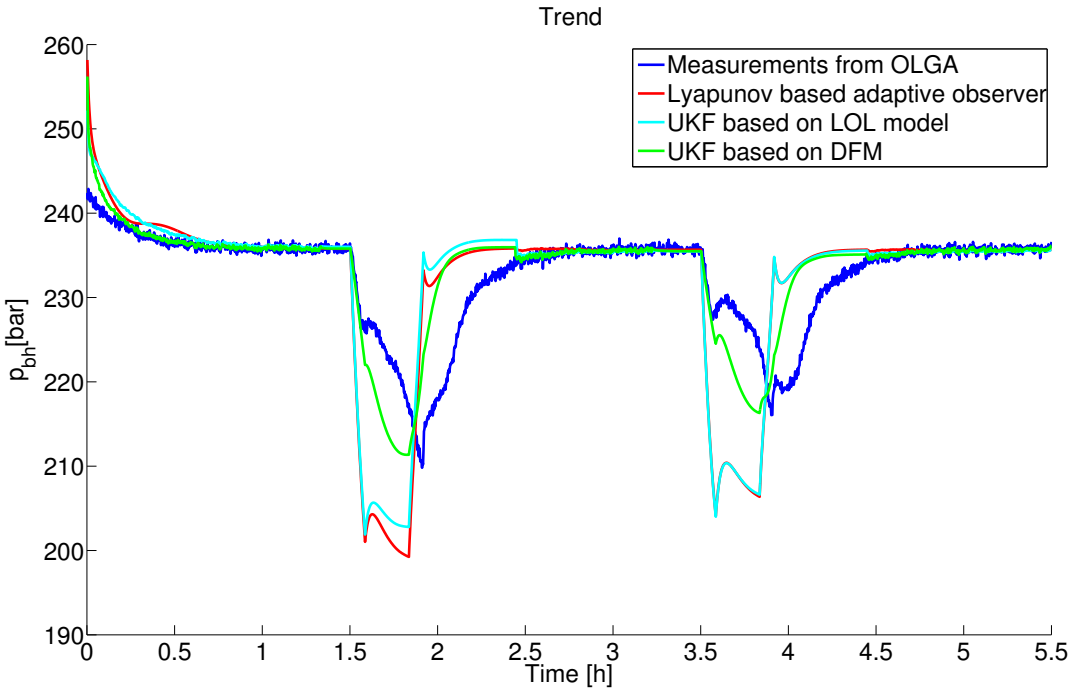

Figure 11: Measured and estimated bottom-hole pressure for pipe connection scenario

6. Conclusion

A simplified DFM and a LOL model describing a multiphase (gas-liquid) flow in the well during UBD has been used. This paper presents the Lyapunov-based adaptive observer and joint UKF based on LOL model for reservoir characterization during UBD operations. Furthermore, it describes a joint UKF to estimate parameters and states for the simplified DFM by using real-time measurements of the choke and the bottom-hole pressures from OLGA simulator. The results show that all estimators are capable of identifying the production constants of gas and liquid from the reservoir into the well. All adaptive observers have a quite fast convergence rate, about 0.5 hour. Simulation results demonstrated reasonable performance of the estimation algorithms to detect and track a changing gas production coefficient using a simulated scenario with OLGA. The nonlinear Lyapunov-based adaptive observer has better accuracy than the other methods for estimation of the production constants of gas and liquid from the reservoir into the well. The adaptive observers based on the LOL model are computationally simpler than joint UKF based on DFM. However, the adaptive observers based on LOL model are more sensitive to errors in the reservoir and well parameters of the model than joint UKF based on DFM.

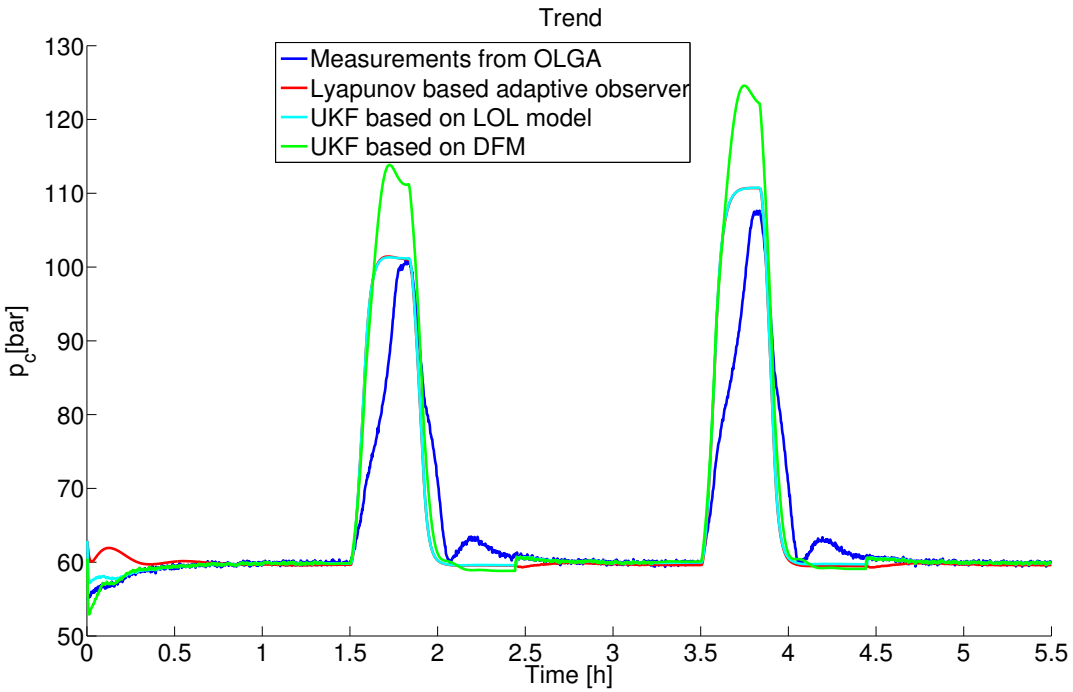

Figure 12: Measured and estimated choke pressure for pipe connection scenario

Acknowledgment

The authors gratefully acknowledge the financial support provided to this project through the Norwegian Research Council and Statoil ASA (NFR project 210432/E30 Intelligent Drilling). We would like to thank Florent Di Meglio, Ulf Jakob Aarsnes, and Agus Hasan for their contribution to the modeling and simulation data.

References

[1] M. Rafique, Underbalanced drilling:" remedy for formation-damage, lost-circulation, and other related conventional-drilling problems", in: SPE Western Regional and Pacific Section AAPG Joint Meeting, 2008.

[2] D. Bennion, F. Thomas, R. Bietz, D. Bennion, Underbalanced drilling, praises and perils, in: Permian Basin Oil and Gas Recovery Conference, 1996.

[3] C. Kardolus, C. van Kruijsdijk, Formation testing while underbalanced drilling, in: SPE annual technical conference, 1997, pp. 521–528.

[4] W. Kneissl, Reservoir characterization whilst underbalanced drilling, in: SPE/IADC drilling conference, 2001, pp. 41–49.

[5] E. H. Vefring, G. Nygaard, R. J. Lorentzen, G. Nævdal, K. K. Fjelde, et al., Reservoir characterization during ubd: Methodology and active tests, in: IADC/SPE Underbalanced Technology Conference and Exhibition, Society of Petroleum Engineers, 2003.

[6] E. H. Vefring, G. H. Nygaard, R. J. Lorentzen, G. Naevdal, K. K. Fjelde, et al., Reservoir characterization during underbalanced drilling (ubd): methodology and active tests, SPE Journal 11 (02) (2006) 181–192.

[7] G. Li, H. Li, Y. Meng, N. Wei, C. Xu, L. Zhu, H. Tang, Reservoir characterization during underbalanced drilling of horizontal wells based on real-time data monitoring, Journal of Applied Mathematics 2014.
[8] G. Nygaard, G. Nævdal, S. Mylvaganam, Evaluating nonlinear kalman filters for parameter estimation in reservoirs during petroleum well drilling, in: Computer Aided Control System Design, 2006 IEEE International Conference on Control Applications, 2006 IEEE International Symposium on Intelligent Control, IEEE, 2006, pp. 1777–1782.
[9] R. Lorentzen, G. Nævdal, A. Lage, Tuning of parameters in a two-phase flow model using an ensemble kalman filter, International Journal of Multiphase Flow 29 (8) (2003) 1283–1309.
[10] G. H. Nygaard, L. S. Imsland, E. A. Johannessen, Using nmpc based on a low-order model for controlling pressure during oil well drilling, in: 8th International IFAC Symposium on Dynamics and Control of Process Systems, Vol. 1, Mexico, 2007, pp. 159–164.
[11] G. Nygaard, G. Nævdal, Nonlinear model predictive control scheme for stabilizing annulus pressure during oil well drilling, Journal of Process Control 16 (7) (2006) 719–732.
[12] A. Nikoofard, T. A. Johansen, G.-O. Kaasa, Nonlinear moving horizon observer for estimation of states and parameters in under-balanced drilling operations, in: ASME 2014 Dynamic Systems and Control Conference, American Society of Mechanical Engineers, 2014.
[13] U. J. F. Aarsnes, O. M. Aamo, F. Di Meglio, G.-O. Kaasa, Fit-for-purpose modeling for automation of underbalanced drilling operations, in: SPE/IADC Managed Pressure Drilling & Underbalanced Operations Conference & Exhibition, Society of Petroleum Engineers, 2014.
[14] A. Nikoofard, U. J. F. Aarsnes, T. A. Johansen, G.-O. Kaasa, Estimation of states and parameters of drift-flux model with unscented Kalman filter, in: Proceedings of the 2015 IFAC Workshop on Automatic Control in Offshore Oil and Gas Production, Vol. 2, Florianópolis, Brazil, 2015, pp. 171–176.
[15] F. Di Meglio, D. Bresch-Pietri, U. J. F. Aarsnes, An adaptive observer for hyperbolic systems with application to underbalanced drilling, in: IFAC World Congress 2014, 2014, pp. 11391–11397.
[16] A. Nikoofard, T. A. Johansen, G.-O. Kaasa, Design and comparison of adaptive estimators for underbalanced drilling, in: American Control Conference (ACC), Portland, Oregon, USA, 2014, pp. 5681–5687.
[17] A. Nikoofard, T. A. Johansen, G.-O. Kaasa, Evaluation of Lyapunov-based adaptive observer using low-order lumped model for estimation of production index in under-balanced drilling, in: 9th International Symposium on Advanced Control of Chemical Processes (ADCHEM), IFAC, Whistler, British Columbia, Canada, 2015, pp. 69–75.
[18] K. H. Bendiksen, D. Maines, R. Moe, S. Nuland, et al., The dynamic two-fluid model olga: Theory and application, SPE production engineering 6 (02) (1991) 171–180.
[19] P. A. Ioannou, J. Sun., Robust adaptive control, Prentice Hall, 1996.
[20] D. Simon, Optimal state estimation: Kalman, H infinity, and nonlinear approaches, Wiley. com, 2006.
[21] E. A. Wan, R. van der Merwe, The Unscented Kalman Filter, in Kalman Filtering and Neural Networks (ed S. Haykin), John Wiley & Sons, New York, USA, 2002, Ch. 7.
[22] A. Hasan, L. Imsland, Moving horizon estimation in managed pressure drilling using distributed models, in: Control Applications (CCA), 2014 IEEE Conference on, IEEE, 2014, pp. 605–610.
[23] B. Rehm, A. Haghshenas, A. S. Paknejad, A. Al-Yami, J. Hughes, Underbalanced Drilling: Limits and Extremes, Elsevier, 2013.
[24] O. M. Aamo, G. Eikrem, H. Siahaan, B. A. Foss, Observer design for multiphase flow in vertical pipes with gas-lift—-theory and experiments, Journal of process control 15 (3) (2005) 247–257.
[25] S. Evje, K. K. Fjelde, Hybrid flux-splitting schemes for a two-phase flow model, Journal of Computational Physics 175 (2002) 674–701.
[26] A. Lage, R. Rommetveit, R. Time, An experimental and theoretical study of two-phase flow in horizontal or slightly deviated fully eccentric annuli, in: IADC/SPE Asia Pacific Drilling Technology, no. 62793-MS, Society of Petroleum Engineers, Kuala Lumpur, Malaysia, 2000.
[27] U. J. F. Aarsnes, F. Di Meglio, S. Evje, O. M. Aamo, Control-oriented drift-flux modeling of single and two-phase flow for drilling, in: ASME 2014 Dynamic Systems and Control Conference, American

Society of Mechanical Engineers, 2014.
[28] E. Storkaas, S. Skogestad, J.-M. Godhavn, A low-dimensional dynamic model of severe slugging for control design and analysis, in: 11th International Conference on Multiphase flow (Multiphase03), 2003, pp. 117–133.
[29] H. K. KHALIL, Nonlinear Systems, 3rd Edition, Prentice Hall, 2002.
[30] S. J. Julier, J. K. Uhlmann, H. F. Durrant-Whyte, A new method for the nonlinear transformation of means and covariances in filters and estimators, IEEE Transactions on Automatic Control 45 (3) (2000) 477–482.
[31] S. J. Julier, J. K. Uhlmann, Unscented filtering and nonlinear estimation, Proceedings of the IEEE 92 (3) (2004) 401 – 422.